Mechanical Performance of Light Weight 3D Printed Interlocked Assemblies

Syed Yasir Hannan [a], Salman Pervaiz [a,*]

[a] *Department of Mechanical and Industrial Engineering, Rochester Institute of Technology –Dubai, Dubai, 341055, United Arab Emirates*
Corresponding author: [*]sxpcad@rit.edu

Abstract— **Topologically interlocked assemblies have traditionally been explored to study properties such as strength, toughness and fatigue when applied axial compressive load. The interlocked assemblies are used in real-life applications ranging from the aerospace industry to the construction sector. This concept is generally applied to segmented blocks to study what parameters affect failure and how the failure occurs. The Segmented interlocked assemblies are investigated to optimize performance and weight compared to a monolithic design with poor strength characteristics. Strength to weight ratio is beneficial to applications where the efficiency of the product relies heavily on the weight. This study is performed on the 3D printed cubes with interlocking geometric slots, and the segmented cubes were investigated for failure through a three-point bending test under different conditions. The study used parameters such as speed of testing, lubrication between blocks, and the shape of the slots. This paper makes use of the Taguchi design of experiments in combination with grey relational analysis to optimize the parameters. Different lubrications were used to create a variation in friction between the blocks simply. After processing the data, it was concluded that the best condition was a circle shape, with lubrication #1 at an indenter speed of 10mm/min, followed by a circle and dry at 5mm/min. Triangle shape with lubrication #1 at a speed of 5mm/min was third in terms of the overall rank. According to the results, the worst-performing condition was a circle shape with lubrication #2 at a 1mm/min speed.**

Keywords— **3D Printed assemblies; bending test; interlocked assemblies.**

I. INTRODUCTION

Alben et al. [1] analyzed the properties of fin rays of fish. In this study, a linear elasticity model was created for the mechanical properties of fish fin rays that predicted the shape of fin rays provided its input muscle actuation and external loading. The study involved simulation and physical experimentation, which involved the measurement of ray deflection at the muscular interface and force-displacement response under actuation. This was carried out with the aid of a micro-CT scan. The simulation model agreed well with an experiment showing the concentrated curvature at the ray base at the point of an externally applied force. Ashby [2] published a study to shed more light on lattice-like structures. The study focused on the effect of properties such as bending and buckling on the thermal and electrical properties of lattice-like structures. Their stress response and bending deformation of the struts that would make up a structure were studied. Some key findings included that stretch-dominated structures have modulus and initial collapse greater than that of a bending dominated cellular structure with similar relative density. Lattice structures showcase unique properties such as low stiffness and strength but the ability to accommodate large strains which also adds an advantage in energy absorption and thermal shock.

Dalaq et al. [3] focused on segmented bodies constructed from stiff blocks subjected to transverse force in another study. The finite element method (FEM) studies the blocks' flexural behavior to forecast strength and the associated toughness. This procedure is used to find the most competent interface geometries and the related interlocking mechanism. The segmented beams were created with ceramic glass by using a laser engraver. The architecture glass reveals that enriched blocks can turn the brittleness of monolithic glass into more gradual deformation that provides a tougher response. It is observed that when compared with the monolithic glass, toughness improved by 370 times and conserved 40% strength. Another study by Djumas et al. [4] analyzed the effect of point loading on different interlocked assemblies structures. The idea was to implement the

knowledge of hierarchical structure to design tunable interlocked assemblies. The deformation mechanics of the structure was simulated on Abaqus software using hyper mesh. The mechanisms of surface contact, namely slip, and tilt were hypothesized to govern the mechanical behavior of interlocked assemblies. The final takeaway from this experiment was that hierarchical structure could contribute significantly to the load-bearing capacity of interlocked geometries, along with the capability of altering the mechanical behavior of interlocked geometries by varying geometrical profiles of the connecting surfaces.

Lattice structural composites are important for functionality in fields such as aerospace. Hu et al. [5] optimized the lattice structural composite inspired by cuttlefish with biomimetics and topology optimization to enhance compressive load-bearing capabilities. A composite made up of carbon fiber was used for structural application. The samples were prepared in the form of blocks that were encouraged by cuttlefish bone. These associated topologies were also improved by computer modeling. The lattice structure provided superior compressive behavior, and stiffness was improved by ten times. Cuttlebone can provide superior compressive strength, enhanced porosity, and impressive permeability, which is of interest in the fields of engineering and biomedical structured materials. Through topology optimization, structural compliance was lessened, and structural stiffness was enhanced. Lattice structure with an optimized performance of Young's modulus is attained at around 26% volume occupied with a relatively low poisons ratio and a topology configuration of 82.5% porosity in the bone structures. David et al. [5] evaluated the parameters affecting the static friction coefficient. The static coefficient friction among materials is a constant value. Tests were carried out to demonstrate the behavior of shear and normal forces needed between contacting surfaces. Thus, there is a need to study stress profiles between contacting surfaces to understand the associated frictional ruptures.

Djumas et al. [6] investigated nacre-inspired materials' performance under the topological interlocking block-based arrangement. The outcomes demonstrated that hybrid structures could be made by combining biomimetic and interlocking approaches. Both approaches were combined using 3D printing-based technology. Design validation was achieved by the experiments using fracture testing. Simulations resulting from finite element analysis computed the equivalent Von-Mises stresses at the crack tip, and revealed regions of stress concentration between interlocking geometries. Thus, the topological interlocking improves composite structures' mechanical properties by preventing elements' brittle failure. Three-dimensional printing technologies such as stereolithography use a scanning laser to build parts layer by layer in a vat of light-cured photopolymer resin. Post-processing process would involve removing excess resin and hardening the object in an oven [7]. Another technique is photopolymer jetting, which uses light-cured resin materials and print heads rather like an inkjet printer laying down layers of photopolymer that would be light-cured. These technologies allow the creation of complex shapes and high-quality finishes, making them ideal for dentistry applications [7].

Tee et al. [8] studied porcupine quills with the aid of biomimicry. In this research paper, the compression properties of porcupine's quill were obtained and compared with the literature-based analytical solution. This was done because a porcupine's quill is a natural material that can endure high compression loads. The study used X-ray computed tomography to quantify the microstructures of porcupine's quill before and after experiments. 3D printing methods such as stereolithography are used to print the complex shapes of the quill. Thus, the compression of the whole quill led to a uniform buckling of the outer shell. It has been noticed that CAD design controls the seed number, relative density, and strut length. By having more struts, connectivity can also be enhanced, and stress distribution can be uniform as well. Ramaswamy et al. [9] studied the performance of interlocked adhesive joints. It has been observed that shear strength and work to failure improved by 10% and 130%, respectively. Liong et al. [10] studied the innovative interlocking designing aspects in masonries for construction-related applications. The study was focused on the parametric investigation of curved surfaces.

Mirkhalaf et al. [11] studied how brittle ceramics can be transformed into tough and deformable materials. The property–structure relationship was studied in the study using different testing and imaging techniques. Relationships between architecture, mechanics, and properties in ceramic panels are studied using a combination of testing with stereo imaging, 3D reconstruction, and FEM modeling. It has been observed that replacing a monolithic plate with an interlocking structure provided better fracture and deformation behavior. FEM results showed that the interlocking angle controlled the contacting pressure.

Molokitnov et al. [12] performed bending tests on blocks and assemblies of unique structures. The interlinkable osteomorphic blocks had a dimension of 20 x 20 x 10mm^3 using a material polyurethane mixture in the mold. Aluminum sheets made the rectangular faces of the panels with a thickness of 2mm. Three-point bending tests were performed on a flat sandwich panel under ASTM C393/C393M-06. The study concluded that topological interlocking with segmenting a monolithic sandwich core and osteomorphic blocks made from polyurethane into an assembly remarkably increases its deflection at failure and the energy absorption capability achieved.

Piekarski [13] utilized the concept of geometric interlocking in prefabricated construction slabs. The study used different equilateral geometric shapes such as triangles, hexagons, and rhombi. The study revealed many challenges in the construction. However, there is good potential for 3D printing technology to be used in this regard. Kuznetsov et al. [14] investigated how nozzle diameter and range of layer height can affect the strength of 3D printed material using FDM with PLA material. It has been observed that controlling the geometry of part one can design the desired strength in the structure. When it comes to the strength intra, layer cohesion plays a significant role. They revealed that as layer height increased, the part strength decreased. Also, strength improved when the structure was printed with the larger diameter nozzle.

Frey et al. [15] also investigated a similar concept of bio-inspired interlocking for wooden materials. It has been

observed that elastic modulus was significantly improved. Kuipers et al. [16] developed the performance of an interlaced topographically interlocking lattice using a dual material based material extrusion system. Ultimate tensile strength was investigated using different orientations. The diagonal orientation provided improved strength by improved interlocking. Al-Obaidi et al. [17] revealed that interlocking geometry-related concepts could significantly delay premature bonding rupture. Javan et al. [18] utilized the concept of soft interfaces, such as rubber between interlocked brick structures. Results showed consistency in mechanical character when loaded. Kim and Siegmund [19] investigated the performance of irregular interlocked tessellated geometry. Shi et al. [20] investigated the shear performance of interlocking geometry to improve performance in construction sector. The study proposed empirical formula as well. In another study, Shi et al. [21] investigated the compressive performance of the same interlocking geometry used in the previous work. The study also conducted numerical results and provided a semi-empirical formula to predict the behavior. Prakash et al. [22] studied the interlocked concrete blocks using artificial neural network. The study revealed that ANN model successfully predicted the mechanical behavior.

Weizmann et al. [23] studied the performance of convex interlocking between geometries for construction industries. The results showed higher load-bearing capacity when compared to other regular geometries again. Maurizi et al. [24] investigated the interlocking mechanism using the deep learning method. The study provided new insights into the interlocking mechanisms using data-driven approaches. Wang et al. [25] investigated the interlocking of 3D-angled carbon fibers with an aluminum matrix. Simulated results were found to be in good agreement with the experiments. Mousavian and Casapulla [26] explored interlocking assemblies' structural performance and feasibility using limit analysis. The study provided a useful understanding of structural performance as a function of interlocking geometry. Williams and Siegmund [27] also studied interlocked tiled architecture based on Archimedean and Lavas approaches. It is observed that the area of the smallest tile provided the best prediction about behavior. Aharoni et al. [28] provided an algorithm to optimize topology using a new-density related concept. Fallacara et al. [29] studied the interlocking behavior of the curved morphologies. Zakeri et al. [30] investigated the buckling behavior of plates made up of interlocked geometries. Thus, it has been observed that the buckling load was reduced by increasing the plate length and reducing the plate thickness. However, thickness reduction was more dominant. Xu et al. [31] studied the performance of non-coplanar interlocking geometries in tube-based shapes. It has been observed that interlocking geometries-based tube absorbed higher energy as compared to monolithic structure.

The current study is performed on the 3D printed cubes with interlocking geometric slots, and the segmented cubes were investigated for failure through a three-point bending test under different conditions. The study used parameters such as speed of testing, lubrication between blocks, and the shape of the slots. This paper uses Taguchi design of experiments 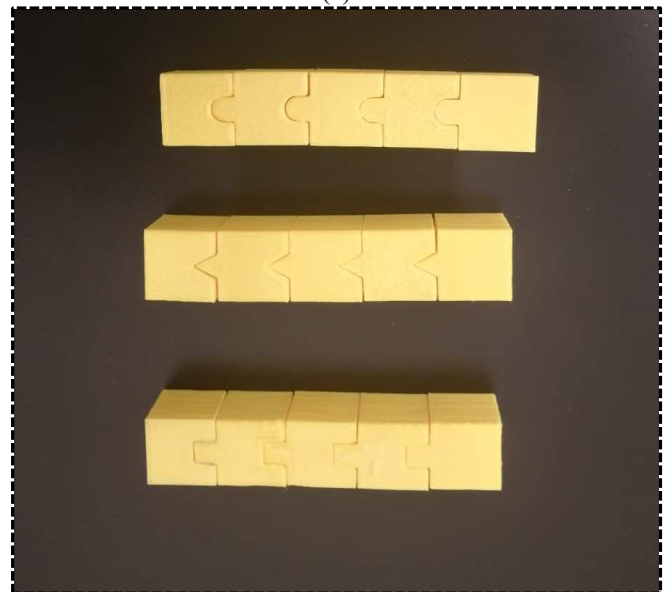in combination with grey relational analysis to optimize the parameters. Different lubrications were used to create a variation in friction between the blocks simply.

II. MATERIALS AND METHOD

The current study focused on measuring parameters such as toughness, ultimate strength, and stiffness using various assemblies of segmented cubes. The authors used different segmented blocks, as shown in Figures 1a and 1b. These blocks have geometric interlocking shapes in the blocks. These interlocking shapes were selected due to the novel and undiscovered potential in the assembly of segmented blocks. The blocks are 25mm x 25mm x 25mm. They were designed on Autodesk inventor and 3d printed using the STL file reader Cura Ultimaker. 3D Printing was performed on Wanhao printers with set parameters shown in Table 1. FDM technology was utilized, and the material for printing was selected as PLA.

(a)

(b)

Fig. 1 (a) 3D printing of blocks (b) Segmented blocks of slots of different shapes (Circle, Triangle, Rectangle)

TABLE I
PRINTING PARAMETERS SET FOR 3D PRINTING THE CUBES

Parameters	Value
Layer Height	0.2mm
Infill Density	20%
Print Speed	40mm/min
Infill Pattern	Grid
Build Plate Adhesion Type	Raft

3D printing took approximately a total time of two days and ten hours for the 25 blocks. The total length of five segmented blocks together came to be around 125.5mm, and this was measured with a Vernier caliper which itself has a tolerance error of +- 0.1 mm. The blocks were placed on a three-point bending test, as seen in Fig. 2, due to lack of load cells on both ends to measure compressive forces. The scale on the Universal Testing Machine was set to be accurate to 125.5mm, implying the blocks were compressed from 0.1 mm from each side, adding up to 0.2mm.
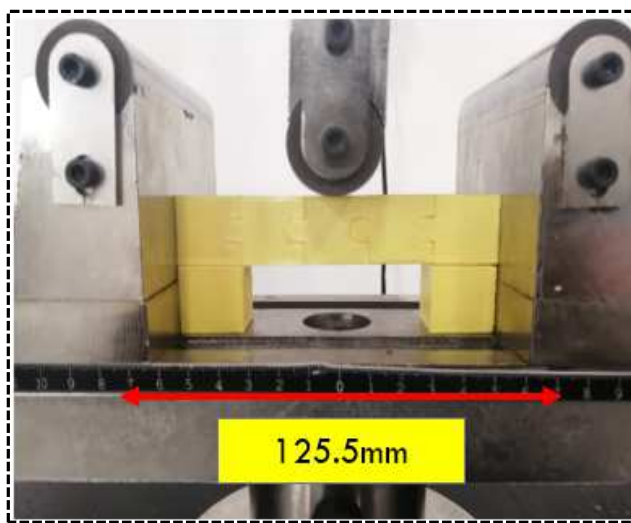

Fig. 2 Setup of three-point bending test for interlocking blocks

The first grease is referred as Lubrication # 1. Lubricant #1 was selected to be AP3 Gel Grease. Lubricant #2 was chosen to MP3 grease. The properties of each one of the lubricants can be found in Table 2. AP grease is Lithium based multifunctional high temperature, water safe oil. MP grease is used mostly in cars and the MP stands for 'Multi-Purpose' (Oil).

TABLE II
PRINTING PARAMETERS SET FOR 3D PRINTING THE CUBES

Properties	AP3 grade (Sterlite Lubricants)	MP3 grade (Mobil Grease)
Soap Type	Lithium	Lithium
Visual Colour	Light Yellow	Medium Brown
Oil viscosity @ 40℃	120	160
Drop Point, °C, min.	190	180
Structure	Smooth and buttery	Smooth

Referring to the table II with properties, it has been noticed that there is a difference in viscosities between the two different kinds of lubricants. Lubricant 1 has a lower Oil viscosity compared to lubricant 2 at a temperature of 40℃.

III. RESULTS AND DISCUSSION

In Taguchi's designs of experiments, a measure of robustness is used to identify control factors that reduce variability in a product or process by minimizing the effects of uncontrollable factors (noise factors). Control factors are those design and process parameters that can be controlled, and noise factors cannot be controlled during production or product use but can be controlled during experimentation. In a Taguchi-designed experiment, as shown in Table III, one can manipulate noise factors to force variability to occur. From the results, identify optimal control factor settings that make the process or product robust or resistant to noise factors. Higher signal-to-noise ratio values (S/N) identify control factor settings that minimize the effects of the noise factors. Due to these reasons, Taguchi was chosen as a method of analysis for the experiment.

TABLE III
TAGUCHI FACTOR DESIGN TABLE WITH 3 INPUT PARAMETERS

Sr. No.	Parameters	L1	L2	L3
1	Shape	Triangle	Rectangle	Circle
2	Lubrication	Dry	Grease 1	Grease 2
3	Speed rate	1mm/min	5mm/min	10mm/min

Minitab 19 was used to compute our factors to help in designing the experiments. Table III shows the factors that we input in 3x3 table. This gave us an L9 orthogonal array, so nine tests would have to be performed as per Taguchi shown in Table IV.

TABLE IV
EXPERIMENTS DESIGNED BY TAGUCHI DESIGN

L1	Triangle	Dry	1
L2	Triangle	Gre1	5
L3	Triangle	Gre2	10
L4	Circle	Dry	5
L5	Circle	Gre1	10
L6	Circle	Gre2	1
L7	Rectangle	Dry	10
L8	Rectangle	Gre1	1
L9	Rectangle	Gre2	5

The data generated by the universal testing machine (UTM) was computed in excel, and the results can be seen in Fig.3. The rows below the graph show how toughness was calculated. To find that we had to find area under the curve, which was done by choosing a second degree polynomial trendline for the curve. The equation generated by excel was later integrated, and the final values were input to find the area in MPa. Ultimate strength was the highest point of the curve, and stiffness using the slope of the linear elastic region.
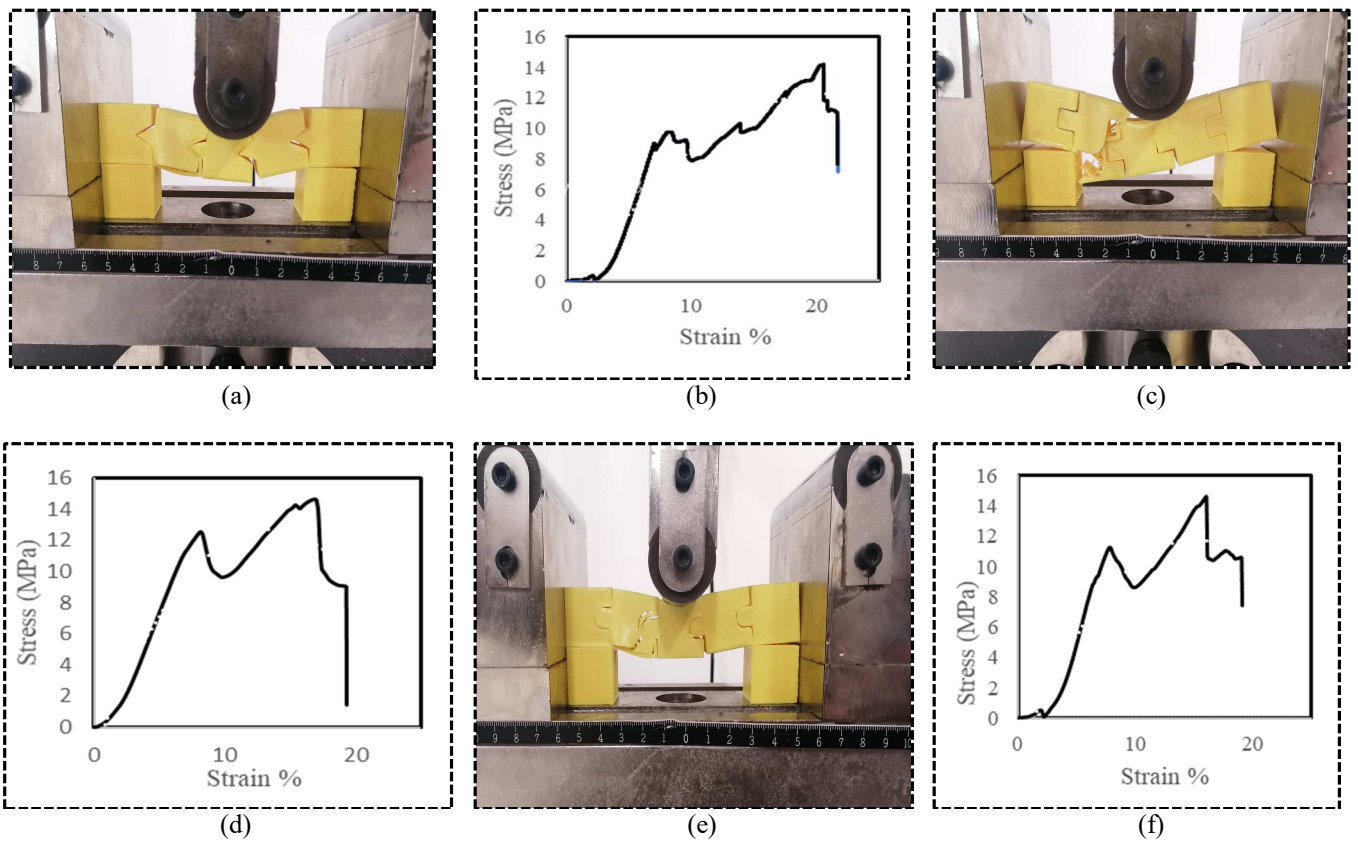
Fig. 3 (a) and (b) Condition 1 -Triangle shape @1mm/min in dry conditions (c) and (d) Condition 4– Rectangle with no Lubrication (dry) @ 10mm/min (e) and (f) Condition 7 – Circle with No lubrication @ 5mm/min

TABLE V
OUTPUT RESULTS OF TAGUCHI DESIGN

Shape	Lubrication	Indenter Speed (mm/min)	Toughness (MPa)	Ultimate Strength (MPa)	Yield Strength (MPa)
Tri	Dry	1	171.68	14.10	2.35
Tri	Gre1	5	203.00	11.38	1.89
Tri	Gre2	10	173.56	11.30	2.30
Cir	Dry	5	152.00	14.58	2.95
Cir	Gre1	10	199.60	14.69	2.52
Cir	Gre2	1	180.00	11.15	1.68
Rec	Dry	10	177.00	14.17	2.19
Rec	Gre1	1	181.93	11.10	1.58
Rec	Gre2	5	187.90	11.81	1.91

Grey relational analysis was implemented in this study to identify the best and most optimized combination of independent variables that yield the best mechanical properties. The Minitab 19 Software was used for Grey Relational Analysis. Grey Relational Analysis was done through a multiple-step sequence, as depicted below in Figure 4. Grey Relational Analysis was done based on the values shown in Table V. For the experiments, the normalized values of original sequence such as toughness, ultimate strength, yield strength, are larger- the better performance characteristic.

$$Xij = \frac{yij - \min(yij)}{\max(yij) - \min(yij)} \qquad (1)$$

The deviation sequence of the normalized data is obtained by normalizing the data points between the values of 0 and 1. The deviation sequence is calculated using equation 2, as depicted below.

$$\Delta 0i\ (k) = x0\ (k) - xi\ (k) \qquad (2)$$

The Grey Relational Coefficient is calculated using equation 3. The formula includes the data points from the deviation sequence responses.

$$\varepsilon i\ (k) = \frac{\Delta \min + (\psi * \Delta \max)}{\Delta ij + (\psi * \Delta max)} \qquad (3)$$

The next step is to determine the Grey Relational Grade (GRG). The GRG of each experiment is determined by computing the average of the response variables from the Grey Relational Coefficient Responses. Equation 4 shows the formula used to compute the Grey Relational Grade.

$$\gamma i = \frac{1}{n} \sum_{i=1}^{n}(k) \qquad (4)$$

Tables VI, VII, and VIII display the Grey Relational Analysis steps and the associated ranks.
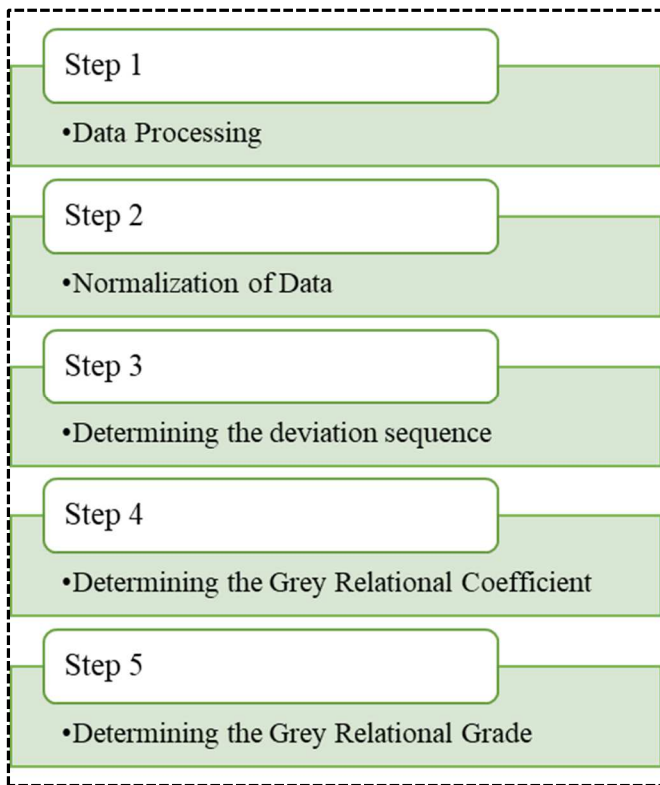
Fig. 4 Multistep Sequence used for Grey Relational Analysis

Step 1
• Data Processing

Step 2
• Normalization of Data

Step 3
• Determining the deviation sequence

Step 4
• Determining the Grey Relational Coefficient

Step 5
• Determining the Grey Relational Grade

TABLE VI
NORMALIZED EXPERIMENTAL RESULTS

Normalized Experimental Results

Toughness	Ultimate Strength	Yield Strength
0.3859	0.8357	0.5639
1.0000	0.0780	0.2314
0.4227	0.0557	0.5309
0.0000	0.9694	1.0000
0.9333	1.0000	0.6884
0.5490	0.0139	0.0732
0.4902	0.8552	0.4453
0.5869	0.0000	0.0000
0.7039	0.1978	0.2417

TABLE VII
DEVIATION SEQUENCING VALUES

Deviation Sequence

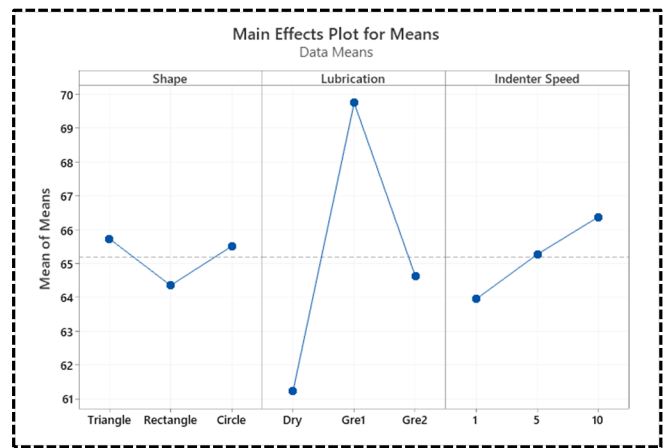| Toughness	Ultimate Strength	Yield Strength
0.6141	0.1643	0.4361
0.0000	0.9220	0.7686
0.5773	0.9443	0.4691
1.0000	0.0306	0.0000
0.0667	0.0000	0.3116
0.4510	0.9861	0.9268
0.5098	0.1448	0.5547
0.4131	1.0000	1.0000
0.2961	0.8022	0.7583

Fig. 5 Plot for Means using Taguchi design

TABLE VIII
RANKING OF EXPERIMENT OUTPUT CONDITIONS

| No. | Grey Relation Coefficient - GRC | | | | |
	Toughness	Ultimate Strength	Yield Strength	Grade	Rank
1	0.4488	0.7526	0.5341	0.578512	5
2	1.0000	0.3516	0.3941	0.581919	3
3	0.4641	0.3462	0.5160	0.442099	7
4	0.3333	0.9423	1.0000	0.75853	2
5	0.8824	1.0000	0.6161	0.832805	1
6	0.5258	0.3365	0.3504	0.404224	9
7	0.4951	0.7754	0.4740	0.581524	4
8	0.5476	0.3333	0.3333	0.404743	8
9	0.6281	0.3840	0.3974	0.469796	6

IV. CONCLUSIONS

The experiment or conditions with the best performance characteristic were noted by referring to the ranks in Table VIII. The larger, the better was selected for all parameters, as the higher the value of toughness, Ultimate Strength, and Yield strength, the better it is. After processing the data, it has been concluded that the best condition was a circle shape, with lubrication 1 (Gre 1) at an indenter speed of 10 mm/min, followed by a circle, Dry, at 5mm/min. Triangle shape with Lubrication 1 at a 5mm/min speed was the third in overall rank. According to our results, the worst performing conditions were circle shape with Lubrication 2 at a speed of 1mm/min.

The study also observed a common trend that the shape circle is the best, followed by a triangle and a rectangle. It has also been noted that the circle shape ranks last, which is again sensitive and subject to other varying parameters. Lubrication 1 is found in one of the top 3 ranks, and Lubrication 2 is among the last, pointing out the role of lubrication in the interlocking process. The study indicates future work to reveal the potential of different lubricants and interlocking geometric shapes to have a tunable desired set of properties such as toughness and flexibility.

REFERENCES

[1] S. Alben, P. G. Madden, and G. V. Lauder, "The mechanics of active fin-shape control in ray-finned fishes," *J. R. Soc. Interface*, vol. 4, no. 13, pp. 243–256, 2007, doi: 10.1098/rsif.2006.0181.
[2] M. F. Ashby, "The Properties of Foams and Lattices," *Philos. Trans. Math. Phys. Eng. Sci.*, vol. 364, pp. 15–30, 2006, [Online]. Available: http://www.jstor.org/stable/25190170.

[3] A. S. Dalaq and F. Barthelat, "Manipulating the geometry of architectured beams for maximum toughness and strength," *Mater. Des.*, vol. 194, p. 108889, 2020, doi: 10.1016/j.matdes.2020.108889.

[4] L. Djumas, G. P. Simon, Y. Estrin, and A. Molotnikov, "Deformation mechanics of non-planar topologically interlocked assemblies with structural hierarchy and varying geometry," *Sci. Rep.*, vol. 7, no. 1, pp. 1–11, 2017, doi: 10.1038/s41598-017-12147-3.

[5] Z. Hu, V. K. Gadipudi, and D. R. Salem, "Topology Optimization of Lightweight Lattice Structural Composites Inspired by Cuttlefish Bone," *Appl. Compos. Mater.*, vol. 26, no. 1, pp. 15–27, 2019, doi: 10.1007/s10443-018-9680-6.

[6] L. Djumas, A. Molotnikov, G. P. Simon, and Y. Estrin, "Enhanced Mechanical Performance of Bio-Inspired Hybrid Structures Utilising Topological Interlocking Geometry," *Sci. Rep.*, vol. 6, no. May, pp. 1–10, 2016, doi: 10.1038/srep26706.

[7] O. Ben-David and J. Fineberg, "Static friction coefficient is not a material constant," *Phys. Rev. Lett.*, vol. 106, no. 25, pp. 1–4, 2011, doi: 10.1103/PhysRevLett.106.254301.

[8] Y. L. Tee, T. Maconachie, P. Pille, M. Leary, T. Do, and P. Tran, "From nature to additive manufacturing: Biomimicry of porcupine quill," *Mater. Des.*, vol. 210, p. 110041, 2021, doi: 10.1016/j.matdes.2021.110041.

[9] K. Ramaswamy, R. M. O'Higgins, M. C. Corbett, M. A. McCarthy, and C. T. McCarthy, "Quasi-static and dynamic performance of novel interlocked hybrid metal-composite joints," *Compos. Struct.*, vol. 253, p. 112769, 2020.

[10] V. Loing, O. Baverel, J. F. Caron, and R. Mesnil, "Free-form structures from topologically interlocking masonries," *Autom. Constr.*, vol. 113, no. September 2019, p. 103117, 2020, doi: 10.1016/j.autcon.2020.103117.

[11] M. Mirkhalaf, A. Sunesara, B. Ashrafi, and F. Barthelat, "Toughness by segmentation: Fabrication, testing and micromechanics of architectured ceramic panels for impact applications," *Int. J. Solids Struct.*, vol. 158, pp. 52–65, 2019, doi: 10.1016/j.ijsolstr.2018.08.025.

[12] A. Molotnikov, R. Gerbrand, O. Bouaziz, and Y. Estrin, "Sandwich panels with a core segmented into topologically interlocked elements," *Adv. Eng. Mater.*, vol. 15, no. 8, pp. 728–731, 2013, doi: 10.1002/adem.201300002.

[13] M. Piekarski, "Floor slabs made from topologically interlocking prefabs of small size," *Buildings*, vol. 10, no. 4, 2020, doi: 10.3390/BUILDINGS10040076.

[14] V. E. Kuznetsov, A. N. Solonin, O. D. Urzhumtsev, R. Schilling, and A. G. Tavitov, "Strength of PLA components fabricated with fused deposition technology using a desktop 3D printer as a function of geometrical parameters of the process," *Polymers (Basel).*, vol. 10, no. 3, 2018, doi: 10.3390/polym10030313.

[15] M. Frey *et al.*, "Tunable Wood by Reversible Interlocking and Bioinspired Mechanical Gradients," *Adv. Sci.*, vol. 6, no. 10, 2019, doi: 10.1002/advs.201802190.

[16] T. Kuipers, R. Su, J. Wu, and C. C. L. Wang, "ITIL: Interlaced Topologically Interlocking Lattice for continuous dual-material extrusion," *Addit. Manuf.*, vol. 50, no. October 2021, p. 102495, 2022, doi: 10.1016/j.addma.2021.102495.

[17] S. Al-obaidi, Y. M. Saeed, and F. N. Rad, "Flexural strengthening of reinforced concrete beams with NSM-CFRP bars using mechanical interlocking," *J. Build. Eng.*, vol. 31, no. August 2019, p. 101422, 2020, doi: 10.1016/j.jobe.2020.101422.

[18] A. R. Javan, H. Sei, X. Lin, and Y. M. Xie, "Mechanical behaviour of composite structures made of topologically interlocking concrete bricks with soft interfaces," vol. 186, 2020, doi: 10.1016/j.matdes.2019.108347.

[19] D. Y. Kim and T. Siegmund, "Materials & Design Mechanics and design of topologically interlocked irregular quadrilateral tessellations," *Mater. Des.*, vol. 212, p. 110155, 2021, doi: 10.1016/j.matdes.2021.110155.

[20] T. Shi, X. Zhang, H. Hao, and G. Xie, "Experimental and numerical studies of the shear resistance capacities of interlocking blocks," *J. Build. Eng.*, vol. 44, no. May, p. 103230, 2021, doi: 10.1016/j.jobe.2021.103230.

[21] T. Shi, X. Zhang, H. Hao, and C. Chen, "Experimental and numerical investigation on the compressive properties of interlocking blocks," *Eng. Struct.*, vol. 228, no. November 2020, p. 111561, 2021, doi: 10.1016/j.engstruct.2020.111561.

[22] K. P. A, J. H. H, and P. O. Awoyera, "Optimization of Mix Proportions for Novel Dry Stack Interlocking Concrete Blocks Using ANN," *Adv. Civ. Eng.*, vol. 2021, p. 15, 2021.

[23] M. Weizmann, O. Amir, and Y. Jacob, "Automation in Construction The effect of block geometry on structural behavior of topological interlocking assemblies," *Autom. Constr.*, vol. 128, no. May, p. 103717, 2021, doi: 10.1016/j.autcon.2021.103717.

[24] M. Maurizi, C. Gao, and F. Berto, "Applications in Engineering Science Interlocking mechanism design based on deep-learning methods," *Appl. Eng. Sci.*, vol. 7, no. May, p. 100056, 2021, doi: 10.1016/j.apples.2021.100056.

[25] Z. Wang, S. Yang, S. Sun, and Y. Zhang, "Multiscale modeling of mechanical behavior and failure mechanism of 3D angle-interlock woven aluminum composites subjected to warp / weft directional tension loading," *Chinese J. Aeronaut.*, vol. 34, no. 8, pp. 202–217, 2021, doi: 10.1016/j.cja.2020.09.016.

[26] E. Mousavian and C. Casapulla, "Structurally informed design of interlocking block assemblages using limit analysis," *J. Comput. Des. Eng.*, vol. 7, no. 4, pp. 448–468, 2020, doi: 10.1093/jcde/qwaa038.

[27] A. Williams and T. Siegmund, "International Journal of Mechanical Sciences Mechanics of topologically interlocked material systems under point load : Archimedean and Laves tiling," *Int. J. Mech. Sci.*, vol. 190, no. April 2020, p. 106016, 2021, doi: 10.1016/j.ijmecsci.2020.106016.

[28] L. Aharoni, I. Bachelet, and J. V Carstensen, "Topology optimization of rigid interlocking assemblies," *Comput. Struct.*, vol. 250, p. 106521, 2021, doi: 10.1016/j.compstruc.2021.106521.

[29] G. Fallacara, M. Barberio, and M. Colella, "Topological Interlocking Blocks for Architecture : From Flat to Curved Morphologies," in *Architectured Materials in Nature and Engineering*, Springer International Publishing, 2019, pp. 423–445.

[30] A. I. Journal, M. Zakeri, M. Majidi, M. Haghighi-yazdi, and M. Safarabadi, "Numerical analysis of linear and nonlinear buckling instability of plates made of topologically interlocked materials," *Mech. Based Des. Struct. Mach.*, vol. 0, no. 0, pp. 1–13, 2021, doi: 10.1080/15397734.2021.1921596.

[31] W. Xu, X. Lin, and Y. M. Xie, "A novel non-planar interlocking element for tubular structures," *Tunn. Undergr. Sp. Technol.*, vol. 103, no. November 2019, p. 103503, 2020, doi: 10.1016/j.tust.2020.103503.